Land Use Policy 75 (2018) 201–214

Contents lists available at ScienceDirect

Land Use Policy

journal homepage: www.elsevier.com/locate/landusepol

# Integrating ecosystem services into effectiveness assessment of ecological restoration program in northern China's arid areas: Insights from the Beijing-Tianjin Sandstorm Source Region

Chong Jiang[a,b,c,*], Reshmita Nath[d,e], Lev Labzovskii[f], Dewang Wang[g]

[a] Guangdong Open Laboratory of Geospatial Information Technology and Application, Guangzhou Institute of Geography, Guangzhou 510070, PR China
[b] Key Lab of Guangdong for Utilization of Remote Sensing and Geographical Information System, Guangzhou 510070, PR China
[c] College of Global Change and Earth System Science, Beijing Normal University, Beijing 100875, PR China
[d] Ministry of Education Key Laboratory for Earth System Modeling, Department of Earth System Science, Tsinghua University, Beijing 100084, PR China
[e] Joint Center for Global Change Studies, Beijing 100875, PR China
[f] Climate Research Division, National Institute of Meteorological Sciences, Jeju-Do, 63568, Republic of Korea
[g] Chinese Research Academy of Environmental Sciences, Beijing 100012, PR China

ARTICLE INFO

*Keywords:*
Beijing–Tianjin Sandstorm Source Region (BTSSR), China
Ecological rehabilitation
Climate variability
Ecosystem service
Synergy

ABSTRACT

The Beijing–Tianjin Sandstorm Source Region (BTSSR) is the main sandstorm source area in northern China, which plays a crucial role in ecological safety and sustainable development of Beijing and the neighbouring areas. As a result of climate change, ecological restoration and anthropogenic activities, the ecosystem in the BTSSR has experienced substantial changes over the recent decades. The main objective of this study is to quantify the dominant ecosystem services from 2000 to 2010, based upon observations and biophysical models. Furthermore, we investigated the role of climatic variability and ecological restoration program in vegetation activity and ecosystem services. Although the slight increase, both in precipitation and temperature during 2000–2010 and despite the implemented ecological rehabilitation, several drought events offset the ecological rehabilitation program. During 2000–2010, both the overall soil conservation and hydrological regulation functions were slightly enhanced. The carbon sequestration remained stable and food production has sharply increased. The increasing rainfall erosivity has intensified water erosion, whereas the reduction in wind speed weakened wind erosion and thereby reduced the sandstorm events. Vegetation restoration induced by the climatic variability and ecological program has also played a positive role in soil conservation and hydrological regulation enhancement. The spatial correlation analysis indicated the synergies between multiple regulating ecosystem services. Moreover, a synergy between food yield and vegetation carbon sequestration (biomass production) has been identified as well. The experience of ecological rehabilitation and ecosystem change in the BTSSR has exemplified the ecological conservation should take climatic variability into account, and facilitate the synergies on multiple ecosystem services in order to maximize the ecosystem's benefits to human well-being.

## 1. Introduction

Ecosystems generate a wide range of services, which are collectively known as the ecosystem services and are important for the well-being of human society (Nelson et al., 2009). Over the past few decades, ecosystem services are one of the central issues in the field of sustainable development and natural resources management research (Dearing et al., 2012). Remarkable progress has been achieved towards the understanding of ecosystem services importance and their associated economic profits (NRC, 2005). There are several underlying drivers for ecosystem service change, which can be summed up as natural and human factors, including policy, economy, technology, and other biophysical conditions (Lü et al., 2012). As a consequence of economic development and population growth, more than half of the worldwide ecosystem has degraded in the last 50 years (MA, 2005). In China, rapid urbanization, farmland expansion, deforestation, reclamation, and other human activities has induced severe environmental degradation on national scale. This degradation in its turn, triggered severe ecological challenges, such as forest degradation, air and soil pollution, water scarcity, desertification, biodiversity loss (SFA, 2010).

Land cover changes induced by anthropogenic and natural factors (i.e., climatic changes) are widely recognized as two major drivers

* Corresponding author at: Guangdong Open Laboratory of Geospatial Information Technology and Application, Guangzhou Institute of Geography, Guangzhou, 510070, PR China.
*E-mail address:* jiangchong1987@mail.bnu.edu.cn (C. Jiang).

https://doi.org/10.1016/j.landusepol.2018.03.018
Received 27 September 2017; Received in revised form 6 March 2018; Accepted 6 March 2018
Available online 05 April 2018
0264-8377/ © 2018 Elsevier Ltd. All rights reserved.

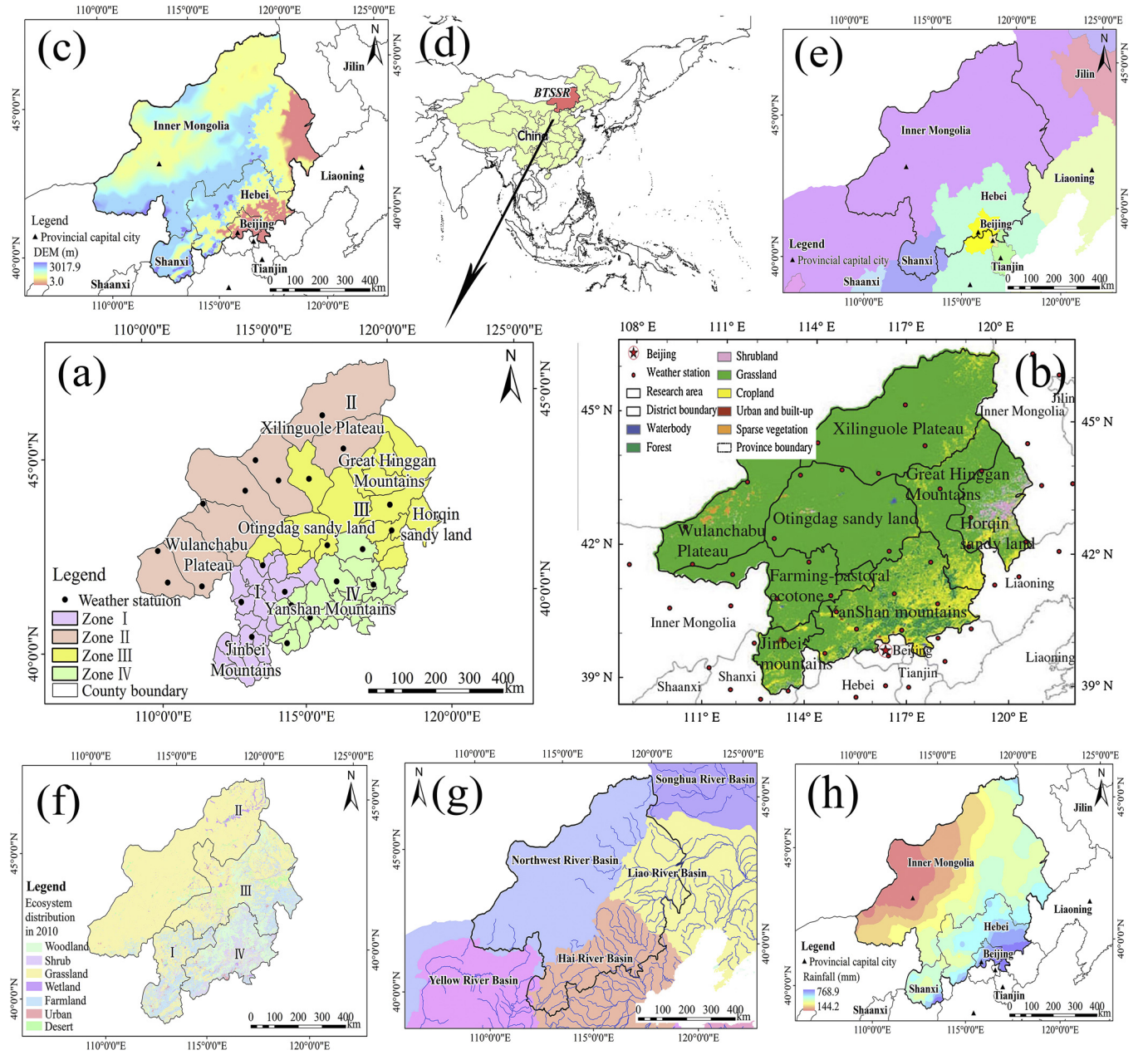


**Fig. 1.** Locations of research area, weather station, and general description of geographical information: (a) spatial distributions of counties, weather stations, and control areas in the BTSSCP. Zone I: control area of arid desert grassland; Zone II: control area of Otingdag sandy land; Zone III: control area of sandy land in the agro-pastoral transition zone; Zone IV: the Yanshan Mountain water source conservation area, (b) geographical zones distribution (Liu et al., 2013), (c) Digital Elevation Model (DEM), (d) location of BTSSR in the world map, (e) administrative divisions in the BTSSR and neighboring areas, (f) ecosystem distribution in 2010, (g) river system distribution, and (h) spatial distribution of years' average rainfall.

influencing the changes in ecosystem and their services (MA, 2005; Nelson et al., 2009). However, the local and global consequences of land cover changes on the ecosystem services and the human society are not clearly understood (Reyers et al., 2009). Effective management of ecosystem services is therefore essential to develop the conservation and land management plans (Kremen, 2005). Furthermore, managing ecosystem services require prior knowledge of their dynamic patterns, status, connections, interactions among the ecosystem structures and functions (MA, 2005). Thereby, a spatially explicit assessment of ecosystem services is critical for making the effective land use and management decisions (Balmford et al., 2002; MA, 2005).

In order to mitigate and adapt to the environmental degradation, in particular for the ecologically fragile regions, a series of ecological restoration programs have been initiated at national and regional scales, e.g., 'Grain for Green Program (GFGP)', 'Three-North Shelterbelt Program (TNSP)', 'Natural Forest Conservation Program (NFCP)', 'Sloping Land Conversion Program (SLCP)', and 'Beijing-Tianjin Sand Source Control Project (BTSSCP)' (Yin and Yin, 2010; Zhang, 2012). These programs are mainly focused on local environmental restoration by planting trees in semi-arid and arid regions, by protecting the natural forests and by encouraging afforestation activities (Zhang et al., 2016). However, the effectiveness of these programs is questioned in the previous studies. It has been reported that the implementation of large scale ecological programs had altered the pattern and the quality of the regional ecosystem. Zhang et al. (2016) reported that the multiple ecological programs accelerated the greening trend in northern China and highlighted the importance of human awareness in regional vegetation growth in the conditions of changing climate. Increasing

trends in vegetation growth have been recently evidenced in other areas as well. These trends were most likely attributed to the large-scale afforestation and reforestation measures (Xu et al., 2014; Sun et al., 2015; Zhao et al., 2015). In addition, vegetation growth in the semiarid regions seems to be highly sensitive to local climate conditions (i.e., evaporation, precipitation, and temperature), and drought significantly affects the vegetation change (Du et al., 2015a,b; He et al., 2015; Qu et al., 2015). In terms of ecosystem service, Lü et al. (2012) investigated the dominant ecosystem services changes from 2000 to 2008 in the Loess Plateau, China, where the ecological rehabilitation program (i.e., GFGP) was launched in 1999. They found that, in the context of climate warming and aridification, the soil conservation and carbon sequestration functions were enhanced, but the water yield was reduced. Wang et al. (2015) assessed the ecosystem services changes in the northeast China from 1992 to 2012, in terms of land cover change and climate variability. They found that the typical trade-offs were presented, which was characterized by an increase in water yield and growth in food production, was in stark contrast with the losses in vegetation carbon stocks and water bird habitats.

BTSSR is the source area for sandstorms in northern China, which is important for the ecological safety and sustainable development of Beijing and the adjoining regions. BTSSR is chosen as the area for our analysis since the first-stage project of the BTSSCP was completed by the end of 2010 (from 2000 to 2010), and it is necessary to assess its effectiveness in regards to alter ecosystem's pattern, quality, and services. Moreover, the previous studies have reported that there was no obvious increasing trend in vegetation activity over the past decade (Liu et al., 2013), and the ecological impacts of vegetation restoration or degradation are still not clear. Therefore, the objectives of this study are (1) to quantify and assess the changes in regulating and provisioning services (i.e., soil conservation, carbon sequestration, hydrological regulation, and food production) from 2000 to 2010 in the BTSSR; (2) to investigate the role of climate variability and ecological restoration program on the vegetation activity and ecosystem services; and (3) to investigate the synergies and trade-offs of multiple ecosystem services, and provide a reference for sustainable development through adaptive management.

## 2. Research area description

The BTSSR (109°30′–119°20′E, 38°50′–46°40′N) is located in the transition region between the Northern China Plain and Mongolia Plateau (Fig. 1a–d) in northern Asia. The extent of BTSSR is bounded by Damao County and Inner Mongolia in the west and extends eastward to Pingyuan County of Hebei Province. In the south it stretches to the Dai County of Shanxi Province and northward to Dong Ujimqin County of Inner Mongolia (Fig. 1a,b,e). As a result, 75 counties (cities or districts) in the provinces of Beijing, Tianjin, Hebei, Shanxi, and Inner Mongolia are included in our analysis, encompassing a total area of $45.93 \times 10^4\,km^2$ (Fig. 1a). The topography transits from plain to plateau (Fig. 1b; Liu et al. (2013)). The plain lands are primarily located in the southeastern part of the BTSSR that forms the part of the Hai River Plain. The altitude of Xilinguole and Bashang plateau reaches its maximum at around 1000 m, with minimum of less than 100 m in Beijing and its surrounding areas (Fig. 1b and c, Wu et al., 2012). The plateau region also includes the Wulanchabu and Xilinguole Plateau. The mountains stretching from the southwest to the northeastern part are located between the plains and the plateaus. The mountains include the northern Taihang, Yanshan, and the southern Greater Hinggan Mountains. The Otingdag and Horqin arid zones are located in the central and eastern part of BTSSR (Fig. 1b). By the assessment from 2010, the BTSSR was territorially composed by $29.57 \times 10^4\,km^2$ of grassland (64.38% of the total area), $5.16 \times 10^4\,km^2$ of woodland (11.23%), $6.63 \times 10^4\,km^2$ of farmland (14.43%), $2.47 \times 10^4\,km^2$ of shrubland (5.38%), and $2.10 \times 10^4\,km^2$ for other types of land uses (4.58%) (Fig. 1f). The BTSSR is located in the transition region of several large river basins of northern China, e.g. the Yellow River Basin, Liao River Basin, Hai River Basin, and Northwest River Basin (Fig. 1g), among which the Northwest River Basin accounts for the largest area.

Being influenced by the atmospheric circulation and local topography, Beijing, Tianjin, and the surrounding regions are exposed to the northerly winds from the Mongolia (SFAC, MA, MWRC, 2001). The region is mainly located in the zone of semi-arid climate and the precipitation is highly contrasting between the southeast and northwestern parts (Fig. 1h). The semi-humid regions of the Miyun and Wutai Mountains receive more than 600 mm of precipitation per year, whereas, the precipitation in the Erlianhaote and Mandula is less than 150 mm per year (Fig. 1h). The annual mean temperature is 6.0 °C, with a spatial pattern of decreasing trend from east to west. Meanwhile, the average number of windy days is 36.2 per year, where the western part is more affected by wind activity than the eastern part of the region. The changes of precipitation spatially consistent with an ecosystem transition from the temperate forest and warm-season vegetation in the southeastern part to the grassland, shrubland, and to the desert in northwestern part (Fig. 1b and f). The vegetation in the west and northwestern parts is mostly represented by grassland and shrubland. Moreover, local vegetation frequently suffers from severe desertification and it is vulnerable to the extreme weather events. In the south and southeastern part, the vegetation cover is spatially more extended and stable due to the substantial amount of planted vegetation (Gao et al., 2008).

The BTSSCP implemented since 2000 is comprised by four subzones including the arid grassland in the north, Otingdag sandy land, the sandy land in the agro-pastoral transition zone, and the Yanshan Mountain water source conservation area. The total investment is estimated to by around 8.5 billion USD, and the comprehensive control measures include the returning of farmland to forest, artificial reforestation, closing hillsides to facilitate afforestation, grassland restoration, headwater conservation, water saving irrigation, watershed management, and the ecological migration. By the end of first-stage project of the BTSSCP (until 2010), the total areas of afforestation, grassland restoration, and watershed management were $1.0 \times 10^5\,km^2$, $1.1 \times 10^5\,km^2$, $2.3 \times 10^4\,km^2$, respectively and the ecological migration program involved $18 \times 10^4$ persons.

## 3. Data collection and methodology

### 3.1. Data collection and processing

The descriptions of the study data used to estimate ecosystem services and related analyses were listed in Table 1. Daily meteorological observations from 29 weather stations in the BTSSR between 1960 and 2010 were obtained from the China Meteorological Administration (CMA; http://cdc.cma.gov.cn). The geographical locations of weather stations are shown in Fig. 1a and specific information of the stations is presented in Supplementary Table 1. In this study, the evapotranspiration ($ET_0$) was estimated by FAO Penman–Monteith Equation, with the input parameters of daily maximum and minimum air temperatures, relative humidity, wind speed, and sunshine duration as shown in Table 1. Missing records in meteorological data were replaced by interpolation from the average value of parameter taken from the same year as observed in the neighboring stations. The annual and seasonal average values of the climatic variables were then calculated from the daily measurements. Regional mean level of the climatic variables has been performed by averaging the values of the stations within the study area. Many studies have reported that the atmospheric circulation indicated by climate indices can control precipitation and temperature and influence the ecosystem to some extent (e.g., Linderholm et al., 2011; Chakravorty et al., 2013; Xiao et al., 2015). In this study, two climatic indices including Pacific Decadal Oscillation (PDO) and Atlantic Multi-decadal Oscillation (AMO) were used to describe certain temporal aspects of the climate variability. The PDO is

**Table 1**
Descriptions of the study data used for estimating ecosystem services.

| Datasets | Data description | Data type | Spatial resolution | Time scale | Data sources and related references |
|---|---|---|---|---|---|
| Climate data | Daily mean temperature; Daily maximum temperature; Daily minimum temperature; Daily rainfall; Daily mean wind speed; Daily sunshine duration; Daily dust event record. | Point | – | 1960–2010 | China Meteorological Administration (CMA; http://cdc.cma.gov.cn/) |
| Climate indices | Pacific Decadal Oscillation (PDO) | Point | – | 1960–2010 | National Oceanic and Atmospheric Administration (NOAA; http://www.esrl.noaa.gov/psd/data/correlation/pdo.data) |
| | Atlantic Multi-decadal Oscillation (AMO) | | | | National Climate Centre (NCC; http://cmdp.ncc-cma.net/Monitoring/cn_index_130.php) |
| DEM (Digital Elevation Model) | Advanced Spaceborne Thermal Emission and Reflection Radiometer, Global Digital Elevation Model (ASTER GDEM) | Raster | 30 m | 2009 | http://www.jspacesystems.or.jp/ersdac/GDEM/E/4.html |
| Soil properties | Soil texture, topsoil sand fraction, topsoil silt fraction, topsoil clay fraction, and topsoil organic carbon | Raster | 1 km | 2000 | Harmonized World Soil Database (HWSD; http://www.isric.org/data/harmonized-world-soil-database-version-10) |
| Land use/cover maps | Land use/cover maps interpreted from Landsat TM/ETM images | Raster | 1 km | 2000, 2005, and 2010 | Global Change Research Data Publishing and Repository (http://www.geodoi.ac.cn/WebEn/doi.aspx?Id=177) (Wu et al., 2014; Ouyang et al., 2015) |
| Normalized Difference Vegetation Index (NDVI) | Moderate-resolution Imaging Spectroradiometer (MODIS) MOD13Q1 product | Raster | 1 km | 2000–2010 | https://lpdaac.usgs.gov/data_access/data_pool |
| Arable land area and grain yield | Arable land area and grain yield for each county | Point | – | 1990–2010 | National Bureau of Statistics (NBS; http://www.stats.gov.cn/) |

defined as the leading principal controller of monthly sea surface temperature anomalies in the North Pacific Ocean, poleward of 20 °N (Xiao et al., 2015). The PDO data over a period of 1960–2010 were extracted from National Oceanic and Atmospheric Administration (NOAA; http://www.esrl.noaa.gov/psd/data/correlation/pdo.data). Regional temperature change can be linked to AMO (e.g., Qian et al., 2016; Luo et al., 2016a, b), yearly data of AMO were downloaded from the website of the National Climate Centre (NCC; http://cmdp.ncc-cma.net/Monitoring/cn_index_130.php).

The Moderate Resolution Imaging Spectroradiometer (MODIS) normalized difference vegetation index (NDVI) images with a resolution of 1 km for 2000–2010 were used to estimate the carbon sequestration. Raster-formatted soil data, i.e., soil texture, depth, type, and other properties of soil, including the proportion of sand, silt, clay and the reference soil depth, were acquired from the Harmonized World Soil Database (http://www.isric.org/data/harmonized-world-soil-database-version-10). They were used to calculate the soil erodibility and plant available water content (PAWC). A digital elevation model (DEM) of 30 m resolution was used to analyze the slope length and slope angle (*LS*) factors for the soil conservation assessment. The land use / cover maps (1: 0.1 million-scale) in 2000, 2005, and 2010 were derived from the Global Change Research Data Publishing and Repository (http://www.geodoi.ac.cn/WebEn/doi.aspx?Id=177) to investigate the land use/cover change (LUCC) (Wu et al., 2014; Ouyang et al., 2015). The arable land area, grain yield, and sandstorm event records are collected from the National Bureau of Statistics (NBS; http://www.stats.gov.cn/) and the CMA (http://cdc.cma.gov.cn), respectively.

### 3.2. Methodology

#### 3.2.1. FAO Penman–Monteith method for $ET_0$ estimation

Parameter $ET_0$ is commonly computed from the weather data as the precise field measurements are rather challenging. The FAO Penman–Monteith method is globally the most reliable and universally accepted method for the $ET_0$ estimation under various climate conditions (e.g. Jhajharia et al., 2012; Tabari et al., 2012). The Penman–-Monteith method (Allen et al., 1998) for calculating the daily $ET_0$ can be expressed as:

$$ET_0 = \frac{0.408(R_n - G) + \gamma(900/(T + 273))U_2(e_s - e_a)}{\Delta + \gamma(1 + 0.34U_2)} \quad (1)$$

where $ET_0$ represents the evapotranspiration at the crop surface (mm $day^{-1}$); $R_n$ and $G$ are the net radiation and soil heat flux density (MJ $m^{-2}$ $day^{-1}$), respectively; $T$ and $U_2$ denote the mean daily air temperature (°C) and wind speed (m $s^{-1}$) at 2 m height, respectively; $e_s$, $e_a$, and $e_s$–$e_a$ are the saturation vapor pressure, actual vapor pressure, and the difference between them (the saturation vapor pressure deficit (kPa)), respectively; $\Delta$ and $\gamma$ stand for the slope of the vapor pressure curve and psychrometric constant (kPa $°C^{-1}$), respectively (Allen et al., 1998; Allen, 2000). Since the soil heat flux is small compared to the $R_n$, especially when the surface is covered by vegetation, and the calculation time steps are 24 h or longer, the $G$ is assumed to be zero.

#### 3.2.2. Vegetation cover change analysis

Fractional Vegetation Cover (*FVC*) is a comprehensive quantitative indicator applied to describe the condition of vegetation (Ivits et al., 2013). A dimidiate pixel model, a simplified linear spectral unmixing method, was adopted to calculate the *FVC* (Ivits et al., 2013). Using this model we have to assume that every pixel contains only two elements of vegetation and soil, which can be represented using the following equation:

$$FVC = (NDVI - NDVI_{soil})/(NDVI_{veg} - NDVI_{soil}) \quad (2)$$

Where $NDVI_{soil}$ and $NDVI_{veg}$ represent the *NDVI* value for pure bare soil and vegetation, respectively. The selections of $NDVI_{soil}$ and $NDVI_{veg}$

mainly depend on the land cover map. Since the vegetation types are different, the $NDVI_{veg}$ represents the mean value of all pure vegetation pixels selected from the high resolution observations in the representative study area. $NDVI_{soil}$ is therefore retrieved from the pure soil pixels, which are detected from the hyperspectral images and compared with the field spectral measurements. The process for *FVC* estimation in details can be found in Zeng, 2000 and Montandon et al. (2007).

### 3.2.3. Ecosystem services assessment and mapping

*3.2.3.1. Soil retention estimated by universal soil loss equation (USLE).* The universal soil loss equation (USLE) (McCool et al., 1997; Renard et al., 1997) was used to estimate soil retention of the ecosystem, which is the most widely used method for soil erosion modelling (Tallis et al., 2011). The input parameters take into account the geomorphology, vegetation, climate, and the management measures. At each pixel, the USLE uses an iterative analysis to estimate the soil erosion and trapping by the downstream vegetation and erosion control practices, which gives the ability of vegetation and soil control practice to capture and retain soil. The soil retention was defined as the soil loss without vegetation cover and soil erosion control minus the soil loss for the current land use/land cover. The assessments were applied to quantify and to reconstruct the annual soil loss for both the situations described above, which can be numerically expressed as

$$\Delta A = A_0 - A_v = R \times K \times L \times S \times (1 - C \times P) \quad (3)$$

where $\Delta A$ is the amount of soil retention ($t\,ha^{-1}\,yr^{-1}$), $A_0$ is the potential soil erosion without vegetation cover ($t\,ha^{-1}\,yr^{-1}$), and $A_v$ is the soil erosion under the current land cover and management conditions ($t\,ha^{-1}\,yr^{-1}$). *R*, *K*, *L*, and *S* represent the rainfall erosivity ($MJ\,mm\,ha^{-1}\,h^{-1}\,yr^{-1}$), soil erodibility ($t\,ha\,h\,ha^{-1}\,MJ^{-1}\,mm^{-1}$), slope length, and slope angle factors, respectively. *C* and *P* refer to the vegetation and erosion control factors, respectively. *L*, *S*, *C*, and *P* are dimensionless factors. For the more detailed information on key parameters calibration and localization, please refer to Jiang et al. (2016a, 2016b) and Appendix A.

*3.2.3.2. Sand fixation estimated by revised wind erosion equation (RWEQ).* This study used the revised wind erosion equation (RWEQ) (Fryrear et al., 1998) to assess the sand fixation function of ecosystem. RWEQ is an empirical model used to estimate the long-term soil loss due to wind erosion (Fryrear et al., 2000). Soil movement is expressed by a steady state equation, which assumes the presence of the wind transport capacity. The RWEQ model takes climate, topography, vegetation, soil (e.g., soil erodibility and soil crust) into consideration, and it has been a widely model to quantify wind erosion (Du et al., 2015a,b; Jiang et al., 2015b). The four basic equations involved in the calculation are as follows.

$$\begin{aligned} &\Delta Q = Q_0 - Q_v \\ &Q(x) = Q_{max}\left\{1 - \exp\left[-\left(x/S\right)^2\right]\right\} \\ &Q_{max} = 109.8 \times (WF \times EF \times K \times SCF \times VC) \\ &S = 150.71 \times (WF \times EF \times SCF \times K \times VC)^{-0.3711} \end{aligned} \quad (4)$$

where $\Delta Q$ is the amount of sand fixation ($t\,ha^{-1}\,yr^{-1}$), $Q_0$ is the potential soil erosion without vegetation cover ($t\,ha^{-1}\,yr^{-1}$), and $Q_v$ is the soil erosion under the current land cover and management conditions ($t\,ha^{-1}\,yr^{-1}$). $Q(x)$ is the amount of soil transported by the wind at a point *x*, $Q_{max}$ is the maximum amount of soil that can be transported downwind and *S* is critical field length at which the transported load is 63.2% of $Q_{max}$. *WF* is the weather factor, *EF* is the erodible fraction (aggregates < 0.84 mm), *K*, *SCF*, and *VC* are the soil roughness factor, soil crust factor, and vegetation cover factor, respectively. More detailed information on the key parameters calibration and localization are available in the Appendix A.

*3.2.3.3. Carbon sequestration assessment.* The *NPP* was calculated based on the Carnegie-Ames-Stanford Approach (CASA) model (Potter et al., 1993), which advocates that the plant productivity is correlated with the photosynthetically active radiation absorbed or intercepted by the green foliage (Monteith et al., 1977; Potter et al., 1993). The CASA model is widely used to estimate the *NPP* in China (Piao et al., 2005; Zhu et al., 2006), which involves the following three basic equations.

$$NPP(x, t) = APAR(x, t) \times \varepsilon(x, t) \quad (5)$$

*NPP*(*x*, *t*) ($gC\,m^{-2}$) and *APAR* (*x*, *t*) ($MJ\,m^{-2}$) is the *NPP* and absorbed photosynthetically active radiation of a pixel at a given location *x* and time *t*, respectively; $\varepsilon$ refers to the actual light use efficiency ($g\,MJ^{-1}$). The annual *NPP* estimated by CASA model in Eq. (5) is the accumulation of monthly values during growing seasons. The detailed procedures to calculate *APAR* and $\varepsilon$ are shown in Eqs. (6) and (7), respectively (Piao et al., 2005).

$$APAR(x, t) = SOL(x, t) \times FPAR(x, t) \times 0.5 \quad (6)$$

$$\varepsilon(x, t) = \varepsilon max \times T\varepsilon 1(x, t) \times T\varepsilon 2(x, t) \times W\varepsilon(x, t) \quad (7)$$

*SOL*(*x*, *t*) ($MJ\,m^{-2}$) and *FPAR*(*x*, *t*) ($MJ\,m^{-2}$) are the total solar radiation and fraction of photosynthetically active radiation at a given location *x* and time *t*, respectively; $\varepsilon_{max}$ refers to the maximum light-use efficiency of vegetation in ideal conditions, which are set as follows, 0.542 $gC\,M^{-1}\,J^{-1}$ for cropland, 0.485 $gC\,M^{-1}\,J^{-1}$ for woodland with high cover, 0.429 $gC\,M^{-1}\,J^{-1}$ for woodland with medium and low cover, 0.413 $gC\,M^{-1}\,J^{-1}$ for grassland with high cover, 0.296 $gC\,M^{-1}\,J^{-1}$ for grassland with medium cover, 0.221 $gC\,M^{-1}\,J^{-1}$for grassland with medium cover, and 0.413 $gC\,M^{-1}\,J^{-1}$ for marsh (Zhu et al., 2006); $T_{\varepsilon 1}(x, t)$, $T_{\varepsilon 2}(x, t)$, and $W_{\varepsilon}(x, t)$ refer to the temperature and moisture stressing coefficients of maximum temperature, minimum temperature, and water on the light-use efficiency, respectively.

The *FPAR* for deriving *NPP* is calculated from a NDVI-based simple ratio (*SR*) (Eqs. (8) and (9)).

$$FPAR = \min\left[\frac{SR - SR_{min}}{SR_{max} - SR_{min}}, 0.95\right] \quad (8)$$

$$SR(x, t) = \frac{1 + NDVI(x, t)}{1 - NDVI(x, t)} \quad (9)$$

Where $SR_{max}$ and $SR_{min}$ are the maximum and minimum values of *SR*, respectively. Independent of vegetation type, $SR_{max}$ is set between 4.14 and 6.17 (Piao et al., 2005); $SR_{min}$ is set to 1.08 for all grid cells (Potter et al., 1993). A complete description of the CASA model can be found in the Piao et al. (2005) and Zhu et al. (2006).

*3.2.3.4. Hydrological regulation assessment.* In this study we deployed the rainfall storage method (Zhao et al., 2004a,b,c) to assess the hydrological regulation function of the ecosystem in the BTSSR.

$$Q_{FMZ} = \begin{cases} P_{FZM} \cdot A_{FZ} & \text{if } P_{FZM} < P'_{FZ} \\ P_{FZM} \cdot R_{FZM} \cdot A_{FZ} & \text{if } P_{FZM} \geq P'_{FZ} \end{cases} \quad (10)$$

$$TQ = \sum_{M=1}^{12} \sum_{F=1}^{j} \sum_{Z=1}^{i} Q_{FMZ} \quad (11)$$

Where *TQ* is the total regulated flow ($m^3$) of the regional ecosystem comparing with bare soil; $Q_{FMZ}$ is the regulated flow ($m^3$) in specific sub-ecosystem; $A_{FMZ}$ is ecosystem area ($m^2$); $P_{FMZ}$ is monthly mean rainfall (mm); $P_{FZ}$' is effective rainfall result in the runoff (mm); $R_{FMZ}$ is the adjustment coefficient of hydrological regulation in the ecosystem; *Z* represents the sub-ecosystem; *i* means number of sub-ecosystem; *M* represents month; *F* is the ecosystem type; *j* donates number of sub-ecosystem type. The adjustment coefficient (*R* factor) is related to the spatial distributions of various ecosystems, vegetation cover, topography, soil properties, and other factors, that are determined according to the conducted experiments and previous research results

in the BTSSR and the neighboring area.

*3.2.3.5. Food provision assessment.* Gross production of the grain products was selected as a proxy for food provisioning service of the BTSSR. The grain production was collected as annual summarized data from the department of statistics for each county.

### 3.2.4. Trend analysis

Linear regression method was applied to detect the trends in time series. The slope of regression indicates the direction and amplitude of temporal change in specific variable. Positive and negative slopes indicate an increasing and a decreasing trend, respectively (Piao et al., 2011). In order to quantify the actual amplitude of change trend, Sen's slope estimator was applied to BTSSR data. If there is a linear trend in the time series, the true slope (change per unit time) could be then estimated using a simple nonparametric procedure developed by Sen (1968). Sen's slope estimator did not require the data to be distributed uniformly. Therefore, it has been gradually applied in vegetation dynamics studies (Fernandes and Leblanc, 2005). The detailed information of Sen's slope estimator is available in the Jiang et al. (2015a) and Appendix A.

### 3.2.5. Correlation analyses between ecosystem services flow and climatic factors

Pearson's correlation analysis was performed grid by grid between ecosystem services flow and climatic factors based on MATLAB software, which can simultaneously return both the correlation coefficient and significant test ($p$-value).

## 4. Results and discussions

### 4.1. LUCC, vegetation cover change, and climate variability

#### 4.1.1. LUCC

During 2000–2010, the land cover pattern was relatively stable in the BTSSR with dominant land cover types such as grassland (63.7%), farmland (14.5%), woodland (11.2%), and the total area of other types accounted for less than 10%. As shown in Table 2, in the first half of the decade (2000–2005), grassland, farmland, desert, and wetland shrank by 2.8%, 0.3%, 0.2%, and 0.1%, respectively, meanwhile, woodland, shrubland, and urban area expanded slightly. In the second half of the decade (2006–2010), all the land cover types expanded slightly (less than 0.5%), except for the grassland, which has increased by 2.4%. In the overall period from 2000 to 2010, no obvious changes happened in the seven land cover categories, which were smaller than 0.5% in each category. The comprehensive control measures of the BTSSCP since 2000 include returning farmland to forest, artificial reforestation, closing hillsides to facilitate afforestation, grassland restoration, and other ecological rehabilitation measures, which therefore compressed the farmland (−0.2%) and enlarged the woodland (0.1%) and shrubland (0.3%). However, the urban area sprawled slightly by 0.3%, which can be attributed to rapid urbanization in the BTSSR.

**Table 2**
Land use cover area and percent changes in the BTSSR from 2000–2010.

| Ecosystem categories | 2000 | 2005 | 2010 | 2000–2005 | 2005–2010 | 2000–2010 |
|---|---|---|---|---|---|---|
| | Unit: $10^3 km^2$ | | | Unit: %mmmm | | |
| Woodland | 51.1 | 51.5 | 51.6 | 0.1 | 0.0 | 0.1 |
| Shrubland | 23.2 | 23.7 | 24.7 | 0.1 | 0.2 | 0.3 |
| Grassland | 297.3 | 284.7 | 295.7 | - 2.8 | 2.4 | - 0.4 |
| Wetland and water body | 7.1 | 6.5 | 6.8 | - 0.1 | 0.1 | - 0.1 |
| Farmland | 67.3 | 65.9 | 66.3 | - 0.3 | 0.1 | - 0.2 |
| Urban land | 5.1 | 5.9 | 6.7 | 0.2 | 0.2 | 0.3 |
| Desert and unused land | 8.0 | 7.2 | 7.6 | - 0.2 | 0.1 | - 0.1 |

Note: The numbers in the bracket indicate changes in percent of land cover.

#### 4.1.2. Vegetation cover change

The vegetation cover in 2000 and 2010 presented decreasing trend from southeast to northwest, as shown in Fig. 2a and b. The greatest vegetation cover lied in the Yanshan and Great Hinggan Mountains, where the total zonal mean vegetation cover was higher than 47%. The lowest values of the vegetation cover are distributed mainly in the Wulanchabu Plateau, Xilinguole Plateau, Horqin and Otingdag sandy land (zonal mean < 18%). According to the comparison of vegetation cover between 2000 and 2010 (Fig. 2c), the vegetation cover has decreased (12.5% in average) mainly in the Otingdag sandy land, western Wulanchabu Plateau, northern Xilinguole Plateau, and Yanshan Mountains regions. The temporal variability of vegetation cover in the BTSSR during 2000–2010 ranged between 21.2% in 2001 and 25.7% in 2003 (mean around 23.7%) (Fig. 2d). The variability in vegetation cover was influenced by both the climate variability and ecological rehabilitation. It is clear that BTSSCP promoted vegetation restoration (vegetation cover increment), however, climate variability has played an important role in vegetation growth in the arid and semi-arid areas (details in Section 5.1).

#### 4.1.3. Climate variability

The Fig. 3 showed the climate variability in the BTSSR from 1960 to 2010. The increasing trend of the annual mean temperature in the recent decade (2000–2010) was consistent to the former period (1960–1999) with slope of 0.04 °C $yr^{-1}$ ($p < 0.001$), and the period mean temperature during 2000–2010 was 1.12 °C higher than former period (1960–1999) (Fig. 3a); The annual mean rainfall during 1960–1999 exhibited weak downward trend ($-0.89$ mm $yr^{-1}$, $p > 0.05$), however, it started to increase since 2000 with a slope of 5.49 mm $yr^{-1}$ ($p > 0.05$), which was fivefold faster than that in the former period (Fig. 3b). Although the rainfall during 2000–2010 resulted in increasing trend, the period mean rainfall was 358.67 mm, which was 41.71 mm smaller than that in the former period (400.38 mm). The trend in $ET_0$ was somewhat similar to the rainfall, which represented downward and upward trends in former and latter periods, respectively. In particular, the downward trend in the former period reached 99% significance level (Fig. 3c). The humidity index exhibited rapid fluctuations in the past decades, however, the trends in both periods did not pass the significance test (Fig. 3d). Basically, regional temperature variability in the Eurasia is normally associated with phase change of AMO, and the frequency and intensity of heat waves correlate with AMO (Qian et al., 2016; Luo et al., 2016a, b). Fig. 3e showed the AMO index in the BTSSR during 2000–2010 presented positive phase with period mean level of 0.26, which was contrast to negative phase from 1960 to 1999 (period mean level was −0.21). Therefore, the annual mean temperature during 2000–2010 was much higher than temperature in the 20th century (1960–1999) (Fig. 3a); Linderholm et al. (2011) and Chen et al. (2013) indicated that the East Asian Monsoon was significantly influenced by ENSO, and the major patterns of summer climate in China were strongly connected with the inter-annual variation of PDO. As shown in Fig. 3f, the PDO index during 2000–2010 presented negative phase with period mean level of −0.72, which was contrast to positive phase from late 1970s to late 1990s (period mean level was 0.33). Generally, the East Asian Summer Monsoon is much weaker during negative PDO phases than positive PDO phases, which brings less rainfall in summer (Chen et al., 2013). Thus, the rainfall in the BTSSR during 2000–2010 was smaller than in the past (Fig. 3b), and the climate in recent decade was relatively drier than before.

### 4.2. Soil conservation assessment

#### 4.2.1. Soil retention assessment

The spatial patterns of soil retention amount in 2000 and 2010

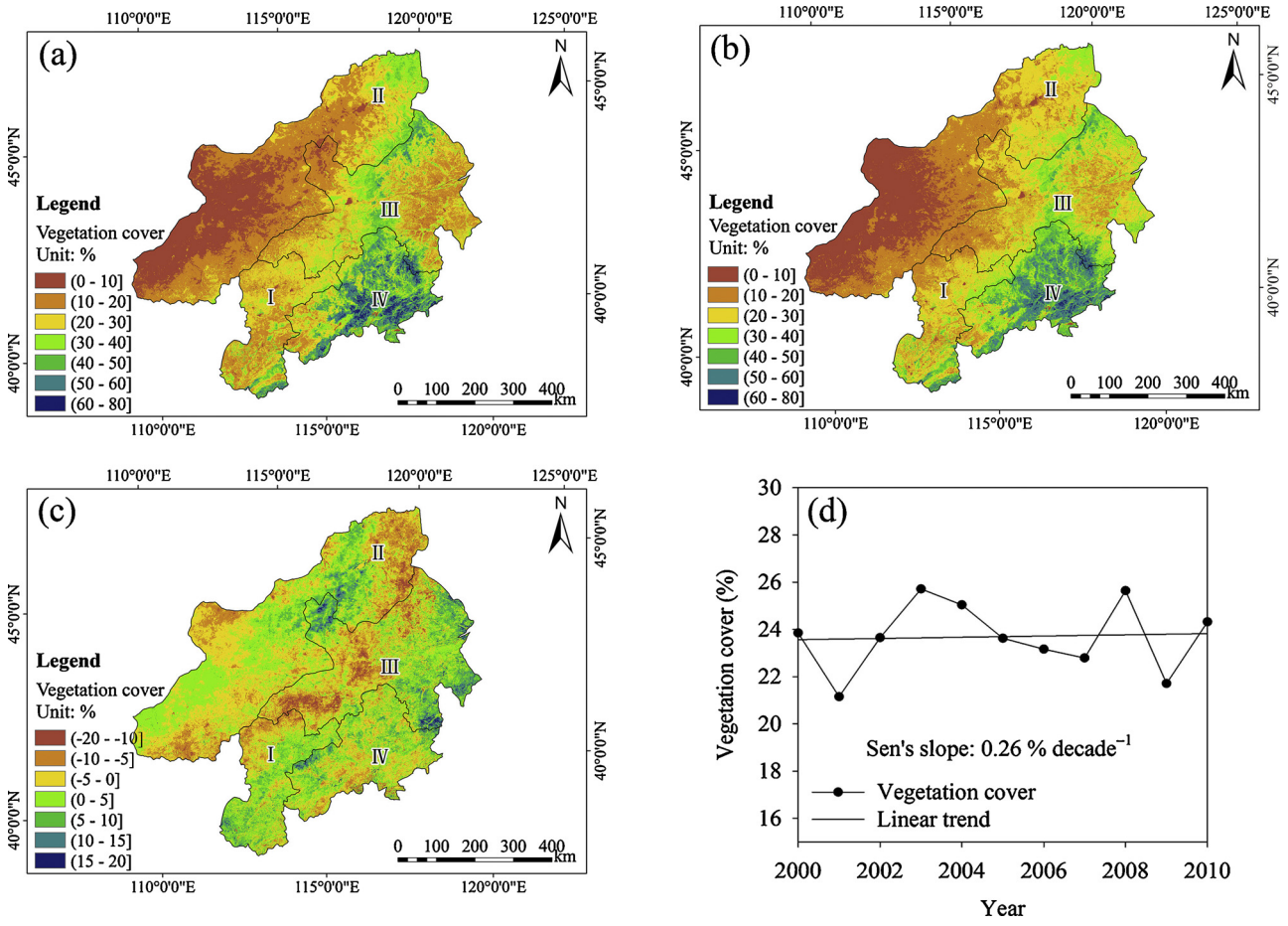


**Fig. 2.** Spatial distributions of vegetation cover in (a) 2000, (b) 2010, (c) difference between 2000 versus 2010, and (d) overall average level change during 2000–2010 in the BTSSR.

represented an obvious spatial heterogeneity with reducing trend from southeast to northwestern part of the BTSSR (Fig. 4a and b). The regional average soil retention amounts in the Yanshan, Jinbei, and Great Hinggan Mountains exceeded 200 t hm$^{-2}$ yr$^{-1}$, which were relatively higher than those in the Wulanchabu Plateau, Xilinguole Plateau, Otingdag sandy land, and neighboring areas (lower than 100 t hm$^{-2}$ yr$^{-1}$). The overall average soil retention amounts in 2000 and 2010 were 50.27 and 50.74 t hm$^{-2}$ yr$^{-1}$, respectively. By comparing the soil conservation amounts between 2000 versus 2010 (Fig. 4c), we found that the areas with reduced soil conservation amount accounted for more than 55%, and were mainly located in the Wulanchabu Plateau, Xilinguole Plateau, Otingdag sandy land, and northern Great Hinggan Mountains. On the other hand, a weak increase can be observed in the Yanshan, Jinbei, and southern Great Hinggan Mountains, which ranged between 5–20 t hm$^{-2}$ yr$^{-1}$. The overall soil retention amount in the BTSSR during 2000–2010 showed slightly increasing trend with a slope of 0.09 t hm$^{-2}$ decade$^{-1}$, but it did not pass the significance test (Fig. 4d). The maximum and minimum soil retention amounts can be seen in 2003 and 2001, with values of 53.64 t hm$^{-2}$ yr$^{-1}$ and 49.80 t hm$^{-2}$ yr$^{-1}$, respectively. The soil retention amount estimated by USLE model depends on six factors, e.g., vegetation cover, rainfall erosivity, topography, soil erodibility. Among them the soil and topographic factors are relatively stable, whereas, the rainfall erosivity and vegetation cover are driven by the natural factor (climate variability) and human activity (ecological restoration, urbanization, etc), respectively. The changes in soil retention amount during 2000–2010 were in accordance with rainfall erosivity and vegetation cover, which are the controlling factors for soil retention (see Section 5.1.1).

#### 4.2.2. Sand fixation assessment

On the aspect of sand fixation amount in the BTSSR, the regional average level in 2000 and 2010 were 34.25 and 34.92 t hm$^{-2}$ yr$^{-1}$, respectively. The sand fixation amounts are relatively large in the Wulanchabu Plateau, Otingdag sandy land, Horqin sandy land, and Yanshan Mountains, see Fig. 5a and b. While comparing the sand fixation amounts between 2000 and 2010 (Fig. 5c), we have found that the area with increasing sand fixation amount accounted for more than 80%, which are mainly distributed in the Yanshan Mountains, Jinbei Mountains, Horqin sandy land, Xilinguole Plateau, and some patches in the Wulanchabu Plateau and Otingdag sandy land. On the other hand, the area in sand fixation amount reduced significantly in the central part of Otingdag sandy land and northwest of the Wulanchabu Plateau, which ranged between $(-20)-(-100)$ t hm$^{-2}$ yr$^{-1}$. The sand fixation amount during 2000–2010 had increased slightly with a slope of 0.73 t hm$^{-2}$ decade$^{-1}$, but it did not exceed the significant level (Fig. 5d). The maximum and minimum amounts were evidenced for 2004 and 2005, with values of 35.56 t hm$^{-2}$ yr$^{-1}$ and 31.10 t hm$^{-2}$ yr$^{-1}$, respectively. The spatial pattern of sand fixation amount in the BTSSR had good consistency with the soil property (soil erodible fraction) map, which showed that the soil property played an important role in the sand fixation ability of the ecosystem. For the temporal variation during 2000–2010, it was directly related to rainfall (soil wetness factor) and vegetation cover (Figs. 2d and 3b).

### 4.3. Carbon sequestration assessment

The spatial pattern of carbon sequestration (NPP) in the BTSSR was shown in Fig. 6a and b. The high NPP area are mainly distributed in the

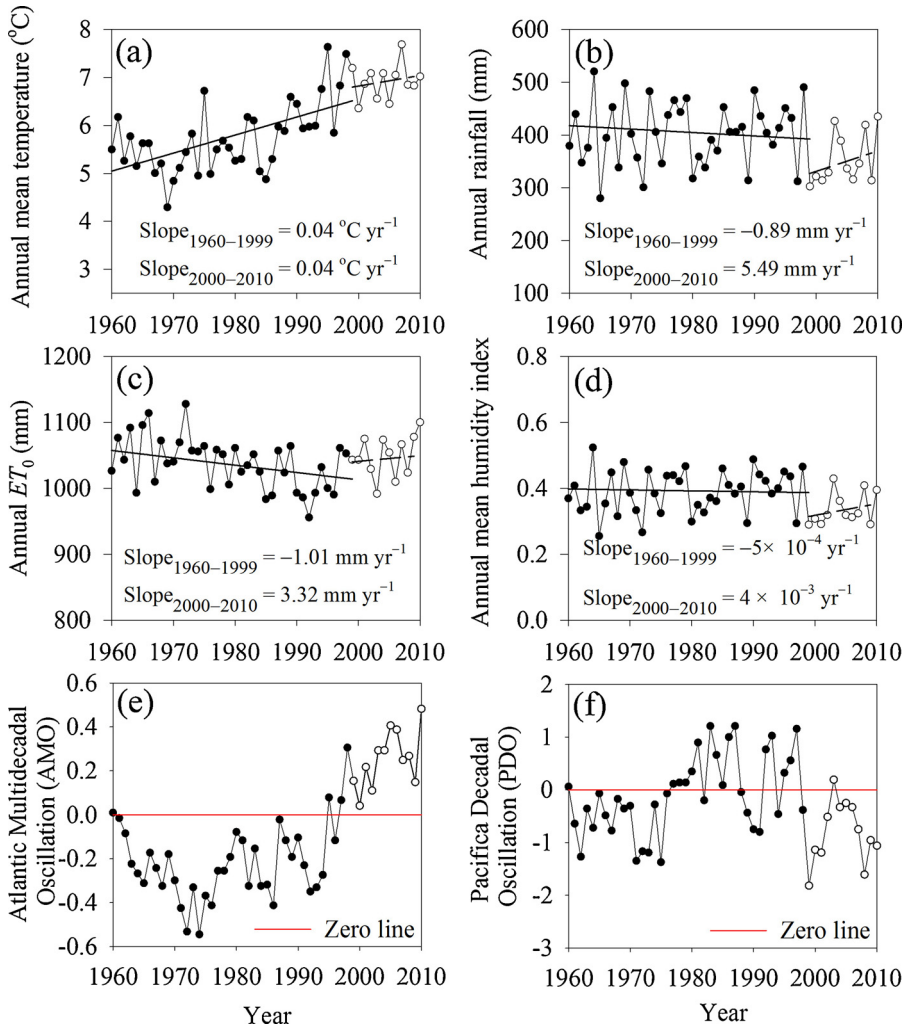


**Fig. 3.** Temporal changes of (a) annual mean temperature, (b) annual rainfall, (c) annual $ET_0$, (d) annual mean humidity index, (e) Atlantic Multi-decadal Oscillation (AMO), and (f) Pacifica Decadal Oscillation (PDO) from 1960 to 2010 in the BTSSR.

Yanshan, Jinbei, and Great Hinggan Mountains, which ranged from 1000 to 2800 gC $m^{-2}$ $yr^{-1}$. NPP decreased from southeast to northwestern part, and the smallest amount (below 300 gC $m^{-2}$ $yr^{-1}$) can be found in the Wulanchabu Plateau, Xilinguole Plateau, Otingdag and Horqin sandy land. We have compared the NPP values between 2000 and 2010 (Fig. 6c), and found that it has decreased mainly in the Otingtag sandy land, Yanshan Mountains, northern Xilinguole Plateau, and Wulanchabu Plateau. In the BTSSR, the NPP values from 2000 to 2010 exhibited large fluctuations, but it did not exert the significant trend (Fig. 6d). The largest (914.3 gC $m^{-2}$ $yr^{-1}$) and the smallest NPP (724.3 gC $m^{-2}$ $yr^{-1}$) values are evidenced in 2005 and 2001, respectively. The changes of NPP in the BTSSR from 2000 to 2010 was in accordance to the changes in rainfall, which is indicative to the fact that the climate conditions represent the dominant factor that affects the vegetation growth, although the ecological rehabilitation had an impact on the vegetation at regional scale (see Section 5.1).

### 4.4. Hydrological regulation assessment

The spatial pattern of the hydrological regulation amounts during 2000 and 2010 exhibited a decreasing trend from the southeast to northwestern part of the BTSSR, with the highest and lowest values were evidenced in the Yanshan Mountains and Wulanchabu Plateau, respectively (Fig. 7a and b). The comparison of hydrological regulation amount between 2000 and 2010 (Fig. 7c) has shown that it has increased slightly from 10 to 70 $m^3$ $hm^{-2}$ $yr^{-1}$ in more than 90% areas considered in the study. A significant increase by 85.21 $m^3$ $hm^{-2}$ $yr^{-1}$ can only be seen in the southernmost part (around Jinbei Mountains) of the BTSSR. The regional average hydrological regulation amount in the BTSSR presented an increasing trend during 2000–2010 with a slope of 21.96 $m^3$ $hm^{-2}$ $decade^{-1}$ ($p > 0.05$) (Fig. 7d). The spatial pattern of hydrological regulation amount in 2000 and 2010 revealed good consistency with rainfall and vegetation cover (Figs. 1h and 2a,b), that are the dominant factors in the hydrological regulation estimation as showed in Section 3.2.3.4. Temporal variation of hydrological regulation amount in its turn was directly related to the rainfall (Fig. 2b). In addition, alterations that changes the hydrological regulation potential (adjustment coefficient $R$ factor) of the ecosystem, such as the conversion of grasslands or the replacement of forests with farmlands or farmlands with the urban areas, can strongly influence the timing and magnitude of runoff, flooding, and aquifer recharge (MA, 2005).

### 4.5. Food production assessment

While comparing the grain yield during the periods of 1990–1999 and 2000–2010 (Fig. 8), the yield in the latter period was lower than the earlier period ($-173.03 \times 10^4$ t), and the arable land area has been also reduced by $49.90 \times 10^4$ ha. We expect that this reduction is the cause of grain yield reduction. Since the implementation of the BTSSCP in 2000, the grain yield in 2001 had reduced largely by $64.21 \times 10^4$ t,

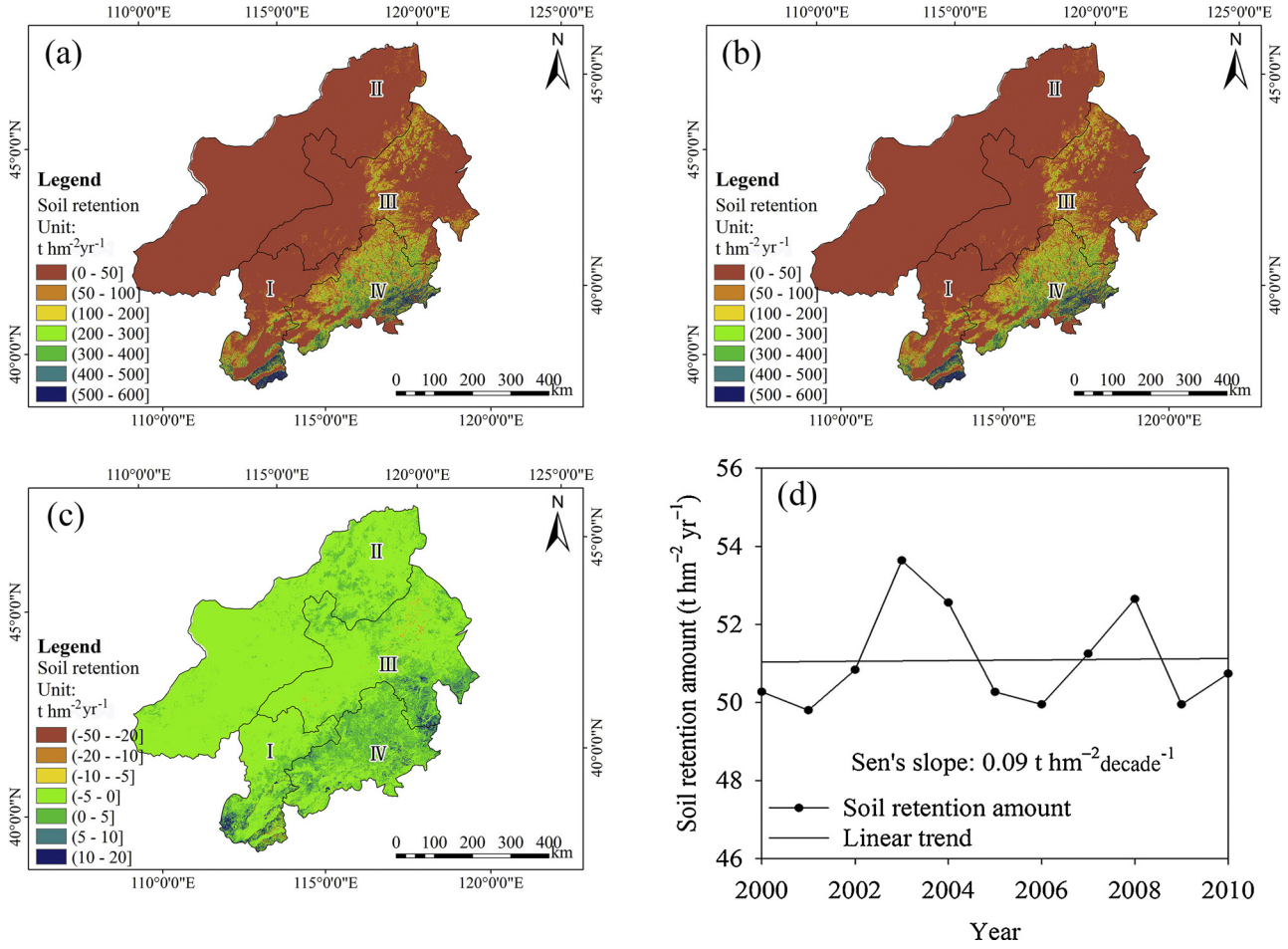


**Fig. 4.** Spatial distributions of soil retention amount in (a) 2000, (b) 2010, (c) difference between 2000 versus 2010, and (d) overall average level change during 2000–2010 in the BTSSR.

which reached the lowest level in the past 20 years i.e. from 1990 to 2010, and then it turned to an increasing trend. The grain yield in 2010 was 1.45 times higher than that in 2001, which correspond to increase of $183.88 \times 10^4$ t in comparison with the grain yield in 2000. In striking contrast, the arable land area in the BTSSR presented a significant decreasing trend during 2000–2010, which reduced by $49.37 \times 10^4$ ha from 2000 to 2010, and the overall level during 2000–2010 was $49.90 \times 10^4$ ha lower than that in 1990–1999. The BTSSCP, therefore, can partly explain the reductions in grain yield and the arable land area. As shown in Fig. 8, the total area of afforestation during 2000–2010 was $1108.59 \times 10^4$ ha. The BTSSCP replaced the arable land with grasslands and woodlands, which had induced a reduction in grain yield in early 2000s. However, with the land use conversion, redistribution of arable land, and development of agricultural technology, the grain yield restored since 2002 and has increased to $800 \times 10^4$ t in 2010, but it was still lower than the mean level in 1990s ($903.75 \times 10^4$ t).

## 5. Driving forces, uncertainties, and implications of ecosystem services changes

### 5.1. Natural and human factors underlying the ecosystem services

#### 5.1.1. Climate variability

Vegetation cover and humidity index were used to reflect the vegetation growth and the climate condition in the BTSSR, respectively (Fig. 9a). Specifically, the vegetation cover in the former half of the decade (2000–2005) showed an increasing trend, whereas it was likely to fluctuate in the latter half of the decade (2006–2010), with a peak value appearing around 2008 and a valley in 2009. Similarly, for the vegetation cover change, the annual mean humidity index from 2000 to 2010, in general, displayed simultaneity with the vegetation cover (Fig. 9a). In 2001, 2007, and 2009, the vegetation cover was relatively low, which was in accordance to the valley region in the humidity index curve. Chen et al. (2013) argued that the East Asian Summer Monsoon was much weaker during negative PDO phases than positive PDO phases, which induced less rainfall. The PDO presented negative phases during 2000–2010 and the rainfall in the BTSSR during 2001, 2007, and 2009 were relatively small (Fig. 3b), thus the climate in these three years were relatively dry comparing with the other years. The relatively dry climate might have contributed to the reduction in vegetation cover in the BTSSR. Similarly, the higher value of humidity index in 2003 and 2008 were coincided with the vegetation cover maxima during the corresponding years; The rainfall erosivity and soil retention amount exhibited a clear correspondence (Fig. 9b). Therefore, the erosion forced by the rainfall increased, which in turn enhanced the soil retention and vice versa. Wind erosion is induced by wind and accompanied by dust event, as shown in Fig. 9c, and the decrease in wind speed since 1985 reduced dust event frequency.

#### 5.1.2. Ecological restoration program

Since 2000, a series of large scale ecological restoration programs have been implemented in the BTSSR and neighboring area, aiming at improving the eco-environment and some of them have exhibited strong positive impacts on the ecosystem (Wu et al., 2012). Specifically, the NFCP aiming at protecting natural forests through logging bans, the

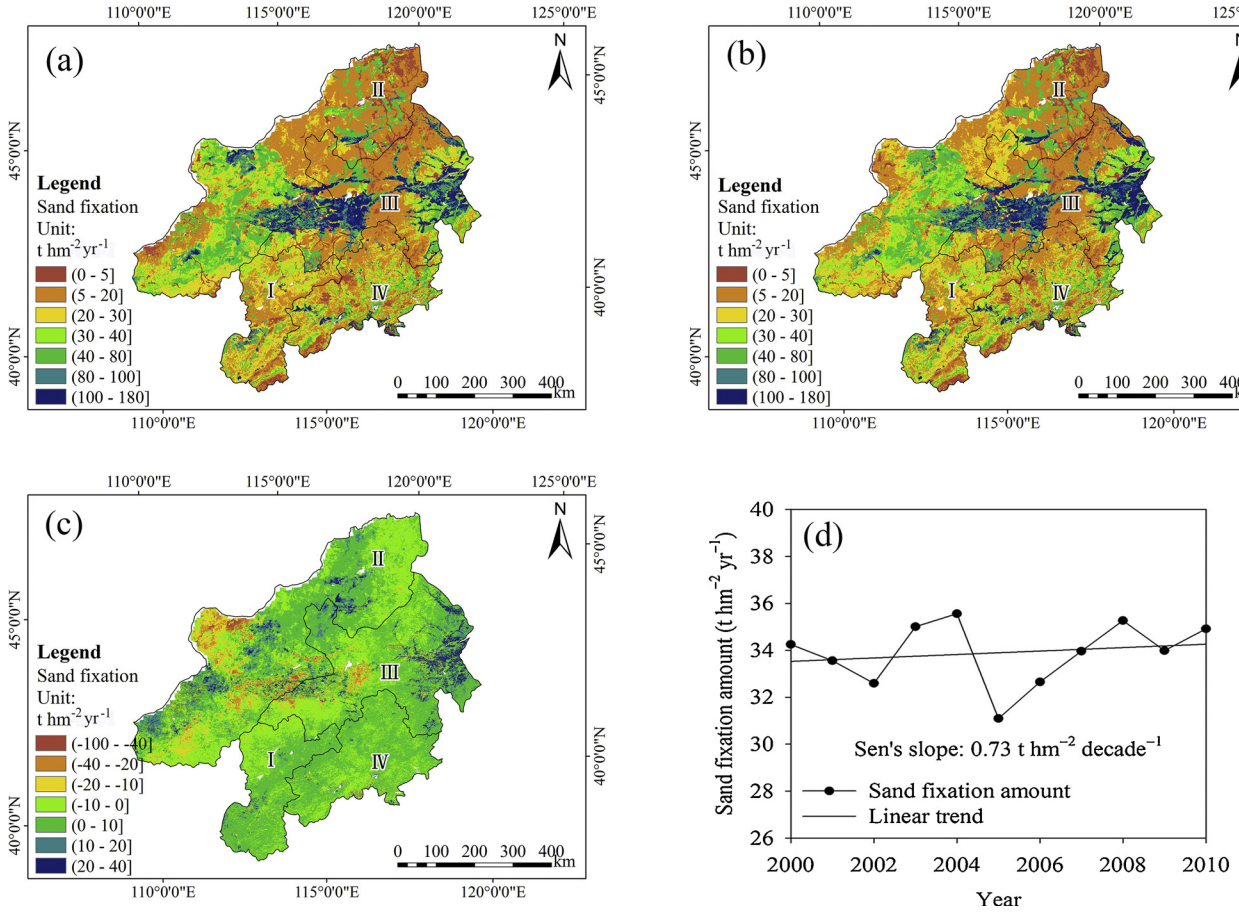


**Fig. 5.** Spatial distributions of sand fixation amount in (a) 2000, (b) 2010, (c) difference between 2000 versus 2010, and (d) overall average level change during 2000–2010 in the BTSSR.

BTSSCP targeting to prevent sandstorms through afforestation, and the GFGP, which targets to convert the farmlands into forests and grasslands, have been implemented in the BTSSR since 2000. The specific measures in the ecological rehabilitation programs involve natural enclosure of grassland, reforestation and afforestation through aerial seeding or closing hill, conversion of the cropland to forest or grassland, and other ecosystem managements. However, there are still some negative effects of unreasonable anthropogenic activities, such as overgrazing, deforestation, and reclamation, which offset the positive effects of the ecological rehabilitation program, even to exploit and destroy the natural ecosystem.

### 5.2. Synergies between ecosystem services

The spatial correlation analysis between multiple ecosystem services in 2000, 2005, 2010, and changes during 2000–2010 suggests that synergies exist between three regulating services in the BTSSR (see Table 3). The ecosystem services are closely linked, being characterized by non-linear relationships (Farber et al., 2002; Van Jaarsveld et al., 2005). These relationships result from trade-offs and synergies across the spatial and temporal scales. Bennett et al. (2009) argued that the ecosystem services were interrelated because of the (1) effects of the common drivers or (2) interactions among the ecosystem services *per se*. In Table 3, the three regulating services were in strong correlation with each other. The correlation can be explained as they are sharing the common biophysical processes and the drivers of climatic and biological factors, such as solar radiation, temperature, precipitation, vegetation cover, etc. Specifically, the positive relationships are evidenced among the soil retention, hydrological regulation, and vegetation carbon sequestration. Evidently, as vegetation recovers (vegetation cover increase), more soil is retained and more water will infiltrate into the soil that in its turn, will increase the regulated runoff. Vegetation restoration or degradation will certainly increase or decrease the carbon sequestration, respectively. Therefore, this study showed positive relationships among the differences in soil retention, hydrological regulation, and carbon sequestration for the BTSSR between 2000 and 2010 (Table 3), indicating the synergies among the three regulating services.

The synergy is evidenced between vegetation carbon sequestration and food production in the BTSSR during 2000–2010 (Figs. 6d and 8). The presence of such synergy draws the agreement with the study conducted by Lü et al. (2012) in the Loess Plateau, China, where the authors have found a synergy between grain production and carbon stocks after GFGP. However, Wang et al. (2015) observed a trade-off between the food production and ecosystem carbon sequestration in the Sanjiang Plain, northeast China. Increase in food production could be attributed to the technical progresses in agriculture, such as application of high-quality breeds and effective cultivation technologies (Luan et al., 2013). In addition to this, human interventions have dramatically increased the food provisioning service by means of agriculture expansion; however, this has resulted in changes to the other services such as water purification and retention (MA, 2005).

### 5.3. Uncertainties in the approaches used to assess ecosystem services

There are some uncertainties exist in the ecosystem service assessment. This study used the USLE model to estimate soil retention amount based upon the rainfall, soil property parameters, and management factors (Tattari et al., 2001). However, the soil retention amount might have been overestimated, due to the omission of local sediment

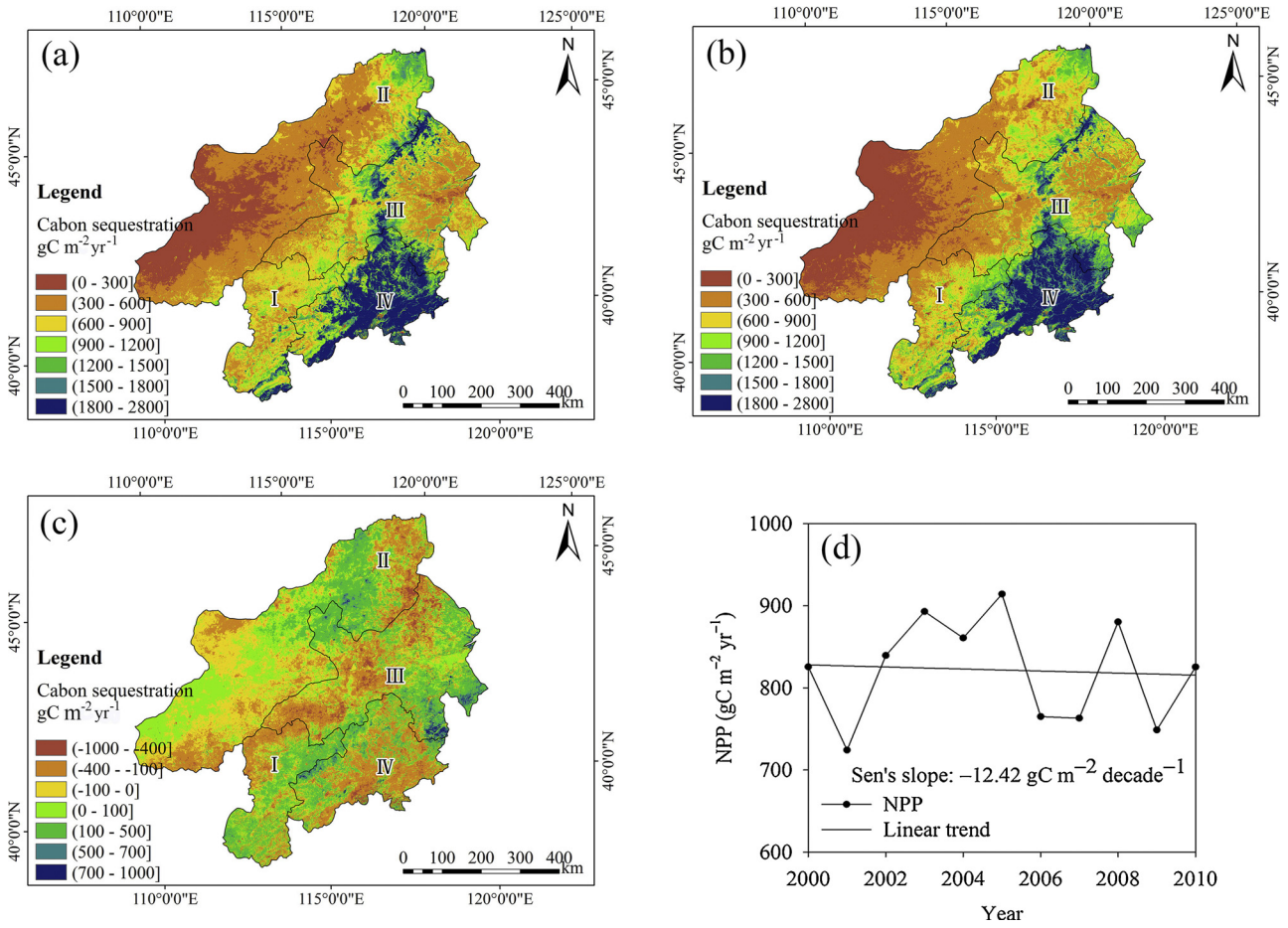


**Fig. 6.** Spatial distributions of carbon sequestration amount (net primary productivity, NPP) in (a) 2000, (b) 2010, (c) difference between 2000 versus 2010, and (d) overall average level change during 2000–2010 in the BTSSR.

deposition and by setting the control for soil retention in a scenario of no vegetation cover or erosion control (Li et al., 2010). Li et al. (2010) used the USLE model to estimate the soil retention amount in the Zuli River Basin, a typical basin in the upstream of Yellow River, which is characterized by severe soil erosion and water scarcity. By comparing the results estimated by USLE with similar soil retention assessments using different methods, they have found a clear overestimation in the simulated result.

Moreover, the estimation of hydrological regulation amount produced new uncertainties. Firstly, the interpolation of an annual mean precipitation from the meteorological data will produce errors. The complex BTSSR terrain represented a challenge to derive the spatial distribution of precipitation, which was interpolated from climatic records of 29 weather stations. Secondly, the adjustment coefficient of the hydrological regulation (*R* factor) is related to the spatial distributions of various ecosystems, vegetation covers, topography factors (e.g., slope, roughness, and aspect), soil properties, and other factors. It is complicated and difficult to quantify and map the spatial variability of these properties. In this study, the *R* factor was simply determined based on the experiments and previous research results in the BTSSR, which have limitations in spatial representation, and therefore will introduce error and uncertainty into estimation result.

In the assessment of vegetation carbon sequestration based on the CASA model, the MODIS data with 1 km resolution and input parameters from national scale studies (Zhu et al., 2006) were used. As we know, the accuracy of estimation result depends largely on the resolution of the remote sensing image and other input data. Moreover, the input parameters on the national scale may not be suitable for local scale studies, due to the limited spatial representation and lack of validations using insitu observations. All the limitations and inaccuracies mentioned above might have introduced errors and uncertainties into the estimation results, which can be somewhat reduced by using finer remote sensing images, more precise soil maps, and localized model parameters.

### 5.4. *Experiences exemplified by ecological rehabilitation and its implications*

The BTSSCP attempted to facilitate the synergies on multiple ecosystem services. These synergies are the important goals which the ecological rehabilitation programs try to reach. The successful performance of the BTSSCP was jointly attributed to the climate variability and the innovative ecosystem management. The BTSSCP struck balance between the provisioning and the regulating services, which provided balanced considerations of the dynamics and sustainability requirements of the targeted ecological-socioeconomic coupled systems. In order to improve the effectiveness of ecological rehabilitation programs, and to mitigate the human disturbance and protect natural ecosystem, an adaptive management paradigm needs to be established to integrate the government motivated “top-down” approach and the local stakeholder motivated “bottom-up” approach (Lü et al., 2012). An adaptive management approach may bring flexibility in human and financial resource allocation, an expansion of knowledge on the dynamic socioeconomic-ecological coupled systems is an urgent need (Gilioli et al., 2007). Currently, the ecological rehabilitation program is widely recognized to be effective tool to reverse the ecological degradation and to mitigate the impacts of climate change on the ecosystem. The performances of BTSSCP and the changes in ecosystem

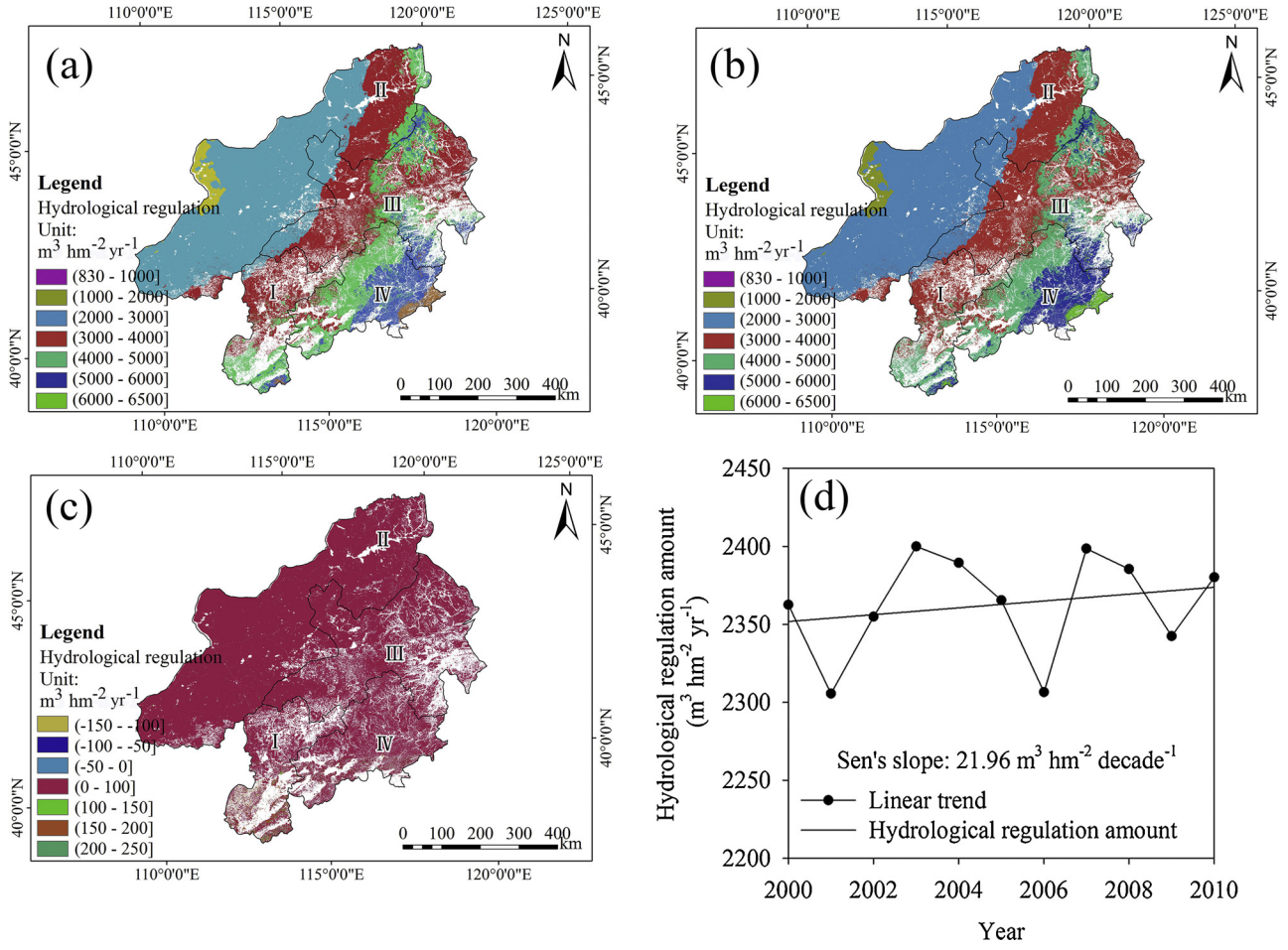


**Fig. 7.** Spatial distributions of hydrological regulation amount in (a) 2000, (b) 2010, (c) difference between 2000 versus 2010, and (d) overall average level change during 2000–2010 in the BTSSR.

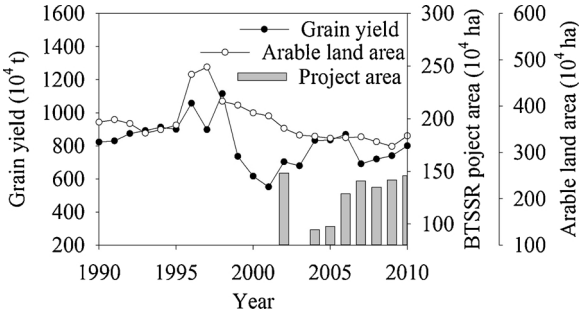


**Fig. 8.** Temporal changes of grain yield and arable land area from 1990 to 2010 and project area during 2002–2010 in the BTSSR.

services exemplifies the positive effects of environmental policies and the necessity of considering climate variability to promote ecological restoration and preserve natural ecosystem in the emerging context of climate change.

## 6. Conclusions

This study quantified and assessed the ecosystem service changes in the BTSSR from 2000 to 2010, in the context of ecological rehabilitation and climate variability, based upon biophysical model simulations and actual observation records. The tradeoffs and synergies between multiple ecosystem services were also analyzed to make the contribution to the improvement of ecosystem management. Although the slight increase in both precipitation and temperature during 2000–2010 and despite the ecological rehabilitation was implemented in the BTSSR, several drought events offset the ecological rehabilitation program and further induced increasing trend in vegetation activity (vegetation cover). The increasing rainfall erosivity throughout 2000–2010 intensified water erosion, and was related to soil retention amount fluctuation. Whereas the reduction in wind speed weakened wind erosion and thereby reduced sandstorm event. Vegetation restoration induced by climate variability and ecological project also played a positive role in soil conservation enhancement. From 2000 to 2010, the overall soil conservation function was slightly enhanced while the hydrological regulation amount increased. The NPP remained stable and food production increased sharply. The spatial correlation analysis indicated synergies between multiple regulating ecosystem services. The synergy has been also observed between food production and vegetation carbon sequestration. The experience of BTSSCP and the change in multiple ecosystem services exemplified the positive effects of environmental policies and once again underlined the necessity of considering climate variability to promote ecological restoration and for natural ecosystem preservation in the emerging context of climate change. The ecological rehabilitation should strive to facilitate synergies on multiple ecosystem services in order to maximize the benefits of ecosystems for sustainable development of human society.

## Acknowlegements

This study is funded by Guangdong Academy of Sciences (GDAS)' Special Project of Science and Technology Development (2017GDASCX–0701). The authors would like to thank the anonymous

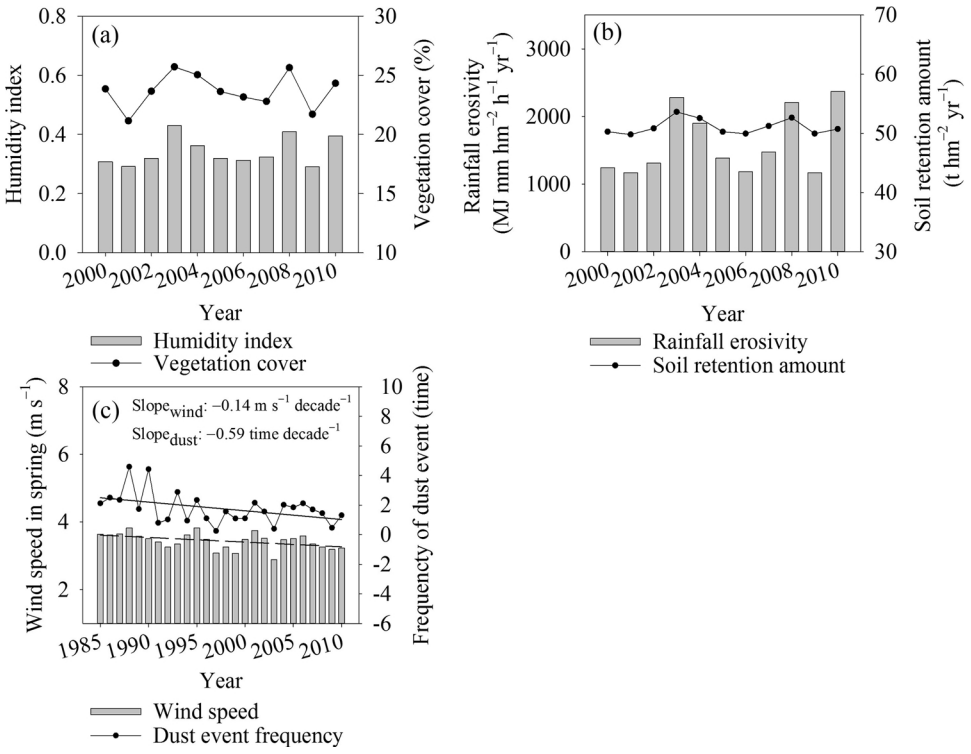


**Fig. 9.** The comparisons of changes in (a) vegetation cover versus humidity index, (b) rainfall erosivity versus soil retention amount from 2000 to 2010, and (c) wind speed in spring versus dust event frequency during 1985–2010 in the BTSSR.

**Table 3**
Correlation analyses between the multiple ecosystem services in the BTSSR.

| Ecosystem service | Period | Hydrological regulation | | | |
|---|---|---|---|---|---|
| | | 2000 | 2005 | 2010 | Change during 2000–2010 |
| Soil conservation | 2000 | 0.559** | - | - | - |
| | 2005 | - | 0.590** | - | - |
| | 2010 | - | - | 0.498* | - |
| | 2000–2010 | - | - | - | 0.505** |
| | | Carbon sequestration | | | |
| | | 2000 | 2005 | 2010 | Change during 2000–2010 |
| Soil conservation | 2000 | 0.694** | - | - | - |
| | 2005 | - | 0.715** | - | - |
| | 2010 | - | - | 0.685** | - |
| | 2000–2010 | - | - | - | 0.566** |
| | | Carbon sequestration | | | |
| | | 2000 | 2005 | 2010 | Change during 2000–2010 |
| Hydrological regulation | 2000 | 0.465* | - | - | - |
| | 2005 | - | 0.525** | - | - |
| | 2010 | - | - | 0.576** | - |
| | 2000–2010 | - | - | - | 0.521** |

* Correlation is significant at the 0.05 level (2-tailed).
** Correlation is significant at the 0.01 level (2-tailed).

reviewers for their helpful and constructive comments and suggestions which have substantially improved the quality of this manuscript.

## Appendix A. Supplementary data

Supplementary material related to this article can be found, in the online version, at doi: https://doi.org/10.1016/j.landusepol.2018.03.018.

## References

Allen, R.G., et al., 1998. Crop Evapotranspiration: Guideline for Computing Crop Water Requirement. FAO Irrigation and Drainage Paper No.56. Food and Agriculture Organisation, Italy.
Allen, R.G., 2000. REF-ET, Reference Evapotranspiration Calculator Version Windows 2.0. User's Manual. University of Idaho Research and Extension Center, Kimberly, ID.
Balmford, A., et al., 2002. Economic reasons for conserving wild nature. Science 297, 950–953.
Bennett, E.M., et al., 2009. Understanding relationships among multiple ecosystem services. Ecol. Lett. 12, 1–11.
Chakravorty, S., Chowdary, J.S., Gnanaseelan, C., 2013. Spring asymmetric mode in the tropical Indian Ocean: role of El Nino and IOD. Clim. Dyn. 40 (5–6), 1467–1481.
Chen, W., Feng, J., Wu, R., 2013. Roles of ENSO and PDO in the link of the East Asian winter monsoon to the following summer monsoon. J. Clim. 26 (2), 622–635.
Dearing, J.A., et al., 2012. Extending the timescale and range of ecosystem services through paleoenvironmental analyses, exemplified in the lower Yangtze basin. Proc. Natl. Acad. Sci. U. S. A. 109, E1111–E1120.
Du, H., et al., 2015a. Assessment of wind-erosion risk in the watershed of the Ningxia-Inner Mongolia Reach of the Yellow River, northern China. Aeolian Res. 17, 193–204.
Du, J., et al., 2015b. Analysis on spatio-temporal trends and drivers in vegetation growth during recent decades in Xinjiang, China. Int. J. Appl. Earth Obs. 38, 216–228.
Farber, S.C., et al., 2002. Economic and ecological concepts for valuing ecosystem services. Ecol. Econ. 41, 375–392.
Fernandes, R., Leblanc, S.G., 2005. Parametric (modified least squares) and nonparametric (Theil-Sen) linear regressions for predicting biophysical parameters in the presence of measurement errors. Remote Sens. Environ. 95 (3), 303–316.
Fryrear, D.W., et al., 1998. Revised Wind Erosion Equation (RWEQ). Wind Erosion and Water Conservation Research Unit, USDA-ARS, Southern Plains area Cropping Systems Research Laboratory. Technical Bulletin No. 1. .
Fryrear, D.W., et al., 2000. RWEQ: improved wind erosion technology. J. Soil Water Conserv. 55 (2), 183–189.
Gao, S., et al., 2008. Benefits of Beijing-Tianjins Sandstorms Source Control Project. Science Press, Beijing, pp. 1–15.
Gilioli, G., et al., 2007. Adaptive eco-social system sustainability enhancement in Sub-Saharan Africa. Ecohealth 4, 428–444.
He, B., et al., 2015. Dynamic response of satellite-derived vegetation growth to climate change in the Three North Shelter Forest Region in China. Remote Sens. 7, 9998–10016.
Ivits, E., et al., 2013. Addressing the complexity in nonlinear evolution of vegetation phenological change with time-series of remote sensing images. Ecol. Indic. 26, 49–60.
Jiang, C., et al., 2015a. Water discharge and sediment load changes in China: change patterns, causes, and implications. Water 7 (10), 5849–5875.
Jiang, L., et al., 2015b. Estimation of wind erosion modules in Qinghai province based on

RWEQ model. Res. Soil Water Conserv. 22 (1), 21–32.
Jiang, C., et al., 2016a. Quantification and assessment of changes in ecosystem service in the Three-River Headwaters Region, China as a result of climate variability and land cover change. Ecol. Indic. 66, 199–211.
Jiang, C., et al., 2016b. Ecosystem change assessment in the Three-river Headwater Region, China: patterns, causes, and implications. Ecol. Eng. 93, 24–36.
Jhajharia, D., et al., 2012. Trends inreference evapotranspiration in the humid region of northeast India. Hydrol. Process. 26 (3), 421–435.
Kremen, C., 2005. Managing ecosystem services: what do we need to know about their ecology? Ecol. Lett. 8, 468–479.
Li, C., et al., 2010. Quantifying the effect of ecological restoration on soil erosion in China's Loess plateau region: an application of the MMF approach. Environ. Manage. 45, 476–487.
Linderholm, H.W., et al., 2011. Interannual teleconnections between the summer North Atlantic Oscillation and the East Asian summer monsoon. J. Geophys. Res. Atmos. 116 D13107.
Liu, J., et al., 2013. Response of NDVI dynamics to precipitation in the Beijing–Tianjin sandstorm source region. Int. J. Remote Sens. 15, 5331–5350.
Lü, Y., et al., 2012. A policy driven large scale ecological restoration: quantifying ecosystem services changes in the Loess Plateau of China. PLoS One 7, e31782.
Luan, Z., et al., 2013. Impacts of intensified agriculture developments on marsh wetlands. Sci. World J. 752846.
Luo, D., et al., 2016a. Impact of Ural blocking on winter warm Arctic–cold Eurasian anomalies. Part I: blocking-induced amplification. J. Clim. 29, 3925–3947.
Luo, D., et al., 2016b. Simmonds, I. Impact of Ural blocking on winter warm Arctic-cold Eurasian anomalies. Part II: The link to the North Atlantic Oscillation. J. Clim. 29, 3949–3971.
McCool, D., et al., 1997. Slope-length and steepness factors (LS). Predicting soil erosion by water: a guide to conservation planning with the Revised Universal Soil Loss Equation (RUSLE). USDA Agriculture Handbook.
MA (Millennium Ecosystem Assessment), 2005. Ecosystems and Human Well-being. Synthesis. Island Press, Washington, DC pp. 1–125.
Montandon, L.M., et al., 2007. The impact of soil reflectance on the quantification of the green vegetation fraction from NDVI. Remote Sens. Environ. 112, 1835–1845.
Monteith, J.L., et al., 1977. Climate and the efficiency of crop production in Britain. Philos. Trans. R. Soc. B 281, 277–294.
Nelson, E., et al., 2009. Modeling multiple ecosystem services, biodiversity conservation, commodity production, and tradeoffs at landscape scales. Front. Ecol. Environ. 7, 4–11.
NRC (National Research Council), 2005. Valuing Ecosystem Service: Towards Better Environmental Decision-making. National Academies Press, Washington, DC pp. 1–200.
Ouyang, Z., et al., 2015. An ecosystem classification system based on remote sensor information in China. Acta Ecol. Sin. 35, 219–226.
Piao, S., et al., 2005. Changes in vegetation net primary productivity from 1982 to 1999 in China. Global Biogeochem. Cycles 19, GB2027. http://dx.doi.org/10.1029/2004CB002274.
Piao, S., et al., 2011. Changes in satellite-derived vegetation growth trend in temperate and boreal Eurasia from 1982 to 2006. Glob. Change Biol. 17, 3228–3239. http://dx.doi.org/10.1111/j. 1365-2486.2011.02419.x.
Potter, C.S., et al., 1993. Terrestrial ecosystem production: a process model based on global satellite and surface data. Glob. Biogeochem. Cy. 7, 811–841.
Qian, W., Wu, K., Leung, J.C., 2016. Three-dimensional structure and long-term trend of heat wave events in western Eurasia revealed with an anomaly-based approach. Int. J. Climatol. 36, 4315–4326.
Qu, B., et al., 2015. Spatio-temporal changes in vegetation activity and its driving factors during the growing season in china from 1982 to 2011. Remote Sens. 7, 13729–13752.
Renard, K.G., et al., 1997. Predicting soil erosion by water: a guide to conservation planning with the Revised Soil Loss Equation (RUSLE). Agriculture Handbook, vol. 703. U.S. Dept. of Agriculture, pp. 404.
Reyers, B., et al., 2009. Ecosystem services, land-cover change, and stakeholders: finding a sustainable foothold for a semiarid biodiversity hotspot. Ecol. Soc. 14, 38.
SFA (State Forestry Administration), 2010. Program Plan of Sandstorm Source Control in Beijing-Tianjin Region. http://english.forestry.gov.cn/web/article.do?action=readnew&id=201001141135256156.
SFAC (the State Forestry Administration of China), MA (Ministry of Agriculture), MWRC (the Ministry of Water Resource of the People's Republic of China), 2001. The Planning of Beijing- Tianjins Sandstorms Source Control Project (2001–2010). http://www.sdpc.gov.cn/ncjj/nczc/t20080414_203913.htm.
Sen, P.K., 1968. Estimates of the regression coefficient based on Kendall's tau. J. Am. Stat. Assoc. 63 (324), 1379–1389.
Sun, W., et al., 2015. Spatiotemporal vegetation cover variations associated with climate change and ecological restoration in the Loess Plateau. Agric. For. Meteorol. 209–210, 87–99.
Tallis, H.T., et al., 2011. InVEST 2.2.2 User's Guide. The Natural Capital Project, Stanford, USA pp. 1–210.
Tabari, H., et al., 2012. Spatial distributionand temporal variation of reference evapotranspiration in arid and semi-aridregions of Iran. Hydrol. Process. 26 (4), 500–512.
Tattari, S., et al., 2001. The concept of sensitivity in sediment yield modelling. Phys. Chem. Earth Part B Hydrol. Oceans Atmos. 26, 27–31.
Van Jaarsveld, A.S., et al., 2005. Measuring conditions and trends in ecosystem services at multiple scales: the Southern African Millennium Ecosystem Assessment (SAfMA) experience. Philos. Trans. R. Soc. B. 360, 425–441.
Wang, Z., et al., 2015. Quantifying changes in multiple ecosystemservices during 1992–2012 in the Sanjiang plain of China. Sci. Total Environ. 514, 119–130.
Wu, B., et al., 2014. Land cover changes of China from 2000 to 2010. Quatern. Sci. 34, 723–731.
Wu, J., et al., 2012. Regional differences in the relationship between climatic factors, vegetation, land surface conditions, and dust weather in China's Beijing-Tianjin Sand Source Region. Nat. Hazards 62, 31–44.
Xiao, M., Zhang, Q., Singh, V.P., 2015. Influences of ENSO, NAO, IOD and PDO on seasonal precipitation regimes in the Yangtze River basin, China. Int. J. Climatol. 35 (12), 3556–3567.
Xu, G., et al., 2014. Changes in vegetation growth dynamics and relations with climate over China's landmass from 1982 to 2011. Remote Sens. 6, 3263–3283.
Yin, R., Yin, G., 2010. China's primary programs of terrestrial ecosystem restoration: initiation, implementation, and challenges. Environ. Manage. 45, 429–441.
Zeng, X., 2000. Derivation and evaluation of global 1-km fractional vegetation cover data for land modeling. J. Appl. Meteorol. 39, 826–839.
Zhang, G., 2012. Effectiveness of ecological restoration projects in Horqin Sandy Land, China based on SPOT-VGT NDVI data. Ecol. Eng. 38, 20–29.
Zhang, Y., et al., 2016. Multiple afforestation programs accelerate the greenness in the 'Three North' region of China from 1982 to 2013. Ecol. Indic. 61, 404–412. http://dx.doi.org/10.1016/j.ecolind.2015.09.041.
Zhao, T., et al., 2004a. Analyses on grassland ecosystem services and its indexes for assessment. Chin. J. Ecol. 23 (6), 155–160.
Zhao, T., et al., 2004b. Ecosystem services and their valuation of China grassland. Acta Ecol. Sin. 24 (6), 1101–1110.
Zhao, T., et al., 2004c. Forest ecosystem services and their valuation in China. J. Nat. Resour. 19 (4), 480–491.
Zhao, X., et al., 2015. Satellite-indicated long-term vegetation changes and their drivers on the Mongolian plateau. Landsc. Ecol. 30, 1599–1611.
Zhu, W., et al., 2006. Simulation of maximum light use efficiency for some typical vegetation types in China. Chin. Sci. Bull. 51 (4), 457–463.